© 2014. Published by The Company of Biologists Ltd | Journal of Cell Science (2014) 127, 3909–3915 doi:10.1242/jcs.155838

SHORT REPORT

The splicing factor U1-70K interacts with the SMN complex and is required for nuclear gem integrity

Eva Stejskalová[1,2] and David Staněk[1,*]

ABSTRACT

The nuclear SMN complex localizes to specific structures called nuclear gems. The loss of gems is a cellular marker for several neurodegenerative diseases. Here, we identify that the U1-snRNP-specific protein U1-70K localizes to nuclear gems, and we show that U1-70K is necessary for gem integrity. Furthermore, we show that the interaction between U1-70K and the SMN complex is RNA independent, and we map the SMN complex binding site to the unstructured N-terminal tail of U1-70K. Consistent with these results, the expression of the U1-70K N-terminal tail rescues gem formation. These findings show that U1-70K is an SMN-complex-associating protein, and they suggest a new function for U1-70K in the formation of nuclear gems.

KEY WORDS: Cajal bodies, Gems, Nuclear structure, SMN, U1 snRNP, U1-70K

INTRODUCTION

The U1 small nuclear ribonucleoprotein particle (U1 snRNP) is an essential component of the spliceosome, a large macromolecular complex responsible for catalyzing pre-mRNA splicing (Will and Lührmann, 2011). The U1 snRNP is composed of the U1 snRNA, a ring of seven Sm proteins and a set of specific proteins – U1A, U1C and U1-70K. U1 snRNA is transcribed by RNA polymerase II and exported to the cytoplasm, where the Sm ring is loaded (Fischer et al., 2011). Sm formation is promoted and controlled by the SMN complex, which consists of the survival of motor neuron (SMN) protein, seven Gemin proteins (Gemin2–Gemin8) and unrip (also known as STRAP) (Fischer et al., 1997; Otter et al., 2007; Cauchi, 2010). After Sm ring assembly and additional maturation steps, the core U1 snRNP is transported back into the nucleus (Fischer and Lührmann, 1990; Neuman de Vegvar and Dahlberg, 1990; Fischer et al., 1993). The SMN complex stays associated with the core snRNP in the cytoplasm and assists during nuclear import (Massenet et al., 2002; Narayanan et al., 2004).

Consistent with its role in snRNP biogenesis, the SMN complex localizes to the cytoplasm. However, the SMN complex is also found in the nucleus, where it accumulates in structures called 'Gemini of Cajal bodies' (gems) (Liu and Dreyfuss, 1996). Nuclear gems are non-membranous bodies distinct from splicing speckles and other structures in the nucleus (Malatesta et al., 2004; Navascues et al., 2004). They often localize adjacent to Cajal bodies, the sites of snRNP modification and processing (Machyna et al., 2013). In addition to the SMN complex proteins, the only additional gem residents identified to date are 'fused in sarcoma' (FUS) and TDP-43, which are both involved in amyotrophic lateral sclerosis (Tsuiji et al., 2013). In addition, the loss of gems correlates with increased severity of spinal muscular atrophy and amyotrophic lateral sclerosis (Shan et al., 2010; Kariya et al., 2012; Achsel et al., 2013).

[1]Department of RNA Biology, Institute of Molecular Genetics AS CR, 142 20 Prague, Czech Republic. [2]Faculty of Science, Charles University in Prague, 128 43 Prague, Czech Republic.

*Author for correspondence (david.stanek@img.cas.cz)

Received 28 April 2014; Accepted 8 July 2014

RESULTS AND DISCUSSION

The U1 snRNP protein U1-70K localizes to nuclear gems and interacts with the SMN complex

It has previously been shown that all major spliceosomal snRNAs, except the U1 snRNA, accumulate in Cajal bodies (Carmo-Fonseca et al., 1991; Matera and Ward, 1993). To better understand the nuclear distribution of the U1 snRNP, we expressed the U1-specific protein U1-70K tagged with GFP in three different cell lines and analyzed its localization with respect to gems and Cajal bodies (supplementary material Fig. S1A). In addition, we used Kyoto HeLa cells stably expressing U1-70K–GFP from a bacterial artificial chromosome, which preserves the endogenous U1-70K promoter and exon-intron structure. In all cell lines, U1-70K–GFP localized to the nucleus and accumulated in distinct foci, which colocalized with nuclear SMN. In cells with separated Cajal bodies and gems, U1-70K–GFP always accumulated in gems and not Cajal bodies, which is consistent with previous findings (Carmo-Fonseca et al., 1991; Matera and Ward, 1993). To avoid possible artifacts of the ectopic expression of U1-70K–GFP, we performed super-resolution microscopy using immunofluorescently labeled endogenous U1-70K. Our data showed that endogenous U1-70K accumulates in gems as well (Fig. 1A). To test whether other components of U1 snRNP are present in gems, we localized U1 snRNA by *in-situ* hybridization and ectopically expressed GFP-tagged U1A and U1C. The U1 snRNA localized to gems, but we did not observe any gem-specific accumulation of either U1A or U1C (Fig. 1A; supplementary material Fig. S1B). To our knowledge, U1-70K is the first example of an snRNP protein accumulating in gems.

To analyze how U1-70K is targeted to gems, we assessed the association of U1-snRNP-specific proteins with the SMN protein. We expressed U1-70K, U1A and U1C tagged with GFP, immunoprecipitated them using anti-GFP antibodies and probed blots for SMN, which specifically co-precipitated with U1-70K–GFP (Fig. 1B). Next, we showed that endogenous U1-70K co-precipitated with all major components of the SMN complex (Fig. 1C), except for unrip, which is known to reside mainly in the cytoplasm (Grimmler et al., 2005). Similar SMN complex proteins were co-purified with ectopically expressed U1-70K–GFP (supplementary material Fig. S2A). The interaction between U1-70K and SMN was RNA independent (supplementary material Fig. S2B), suggesting that U1-70K associated with

Journal of Cell Science

Journal of Cell Science (2014) 127, 3909–3915 doi:10.1242/jcs.155838

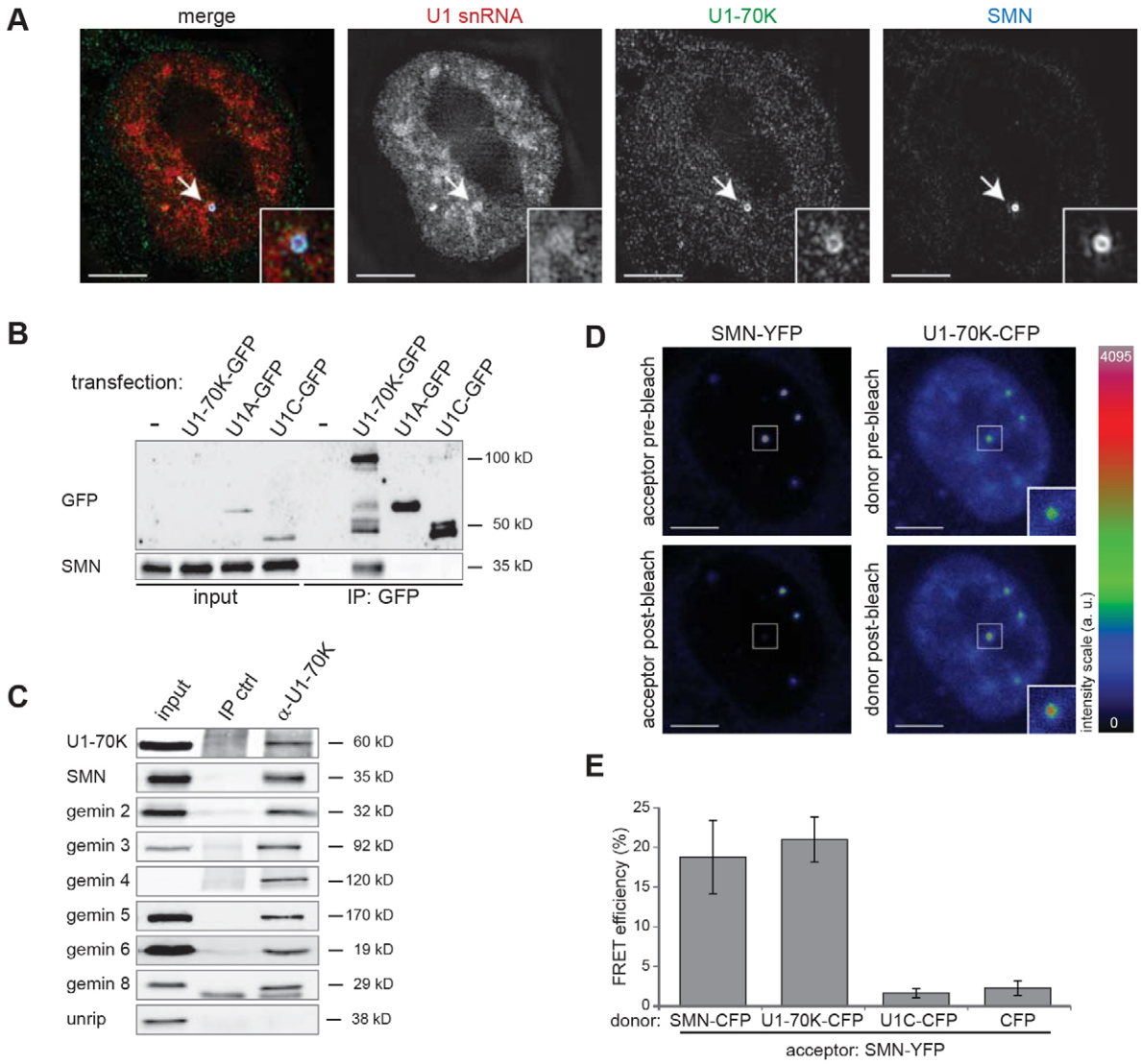

Fig. 1. U1-70K localizes into nuclear gems and interacts with the SMN complex. (A) Super-resolution image of nuclear gems containing SMN protein (blue), U1 snRNA (red) and U1-70K protein (green). The gem marked by the arrow is magnified 2.5× in insets. Scale bars: 5 µm. (B,C) U1-70K interacts with the SMN complex. (B) GFP-tagged U1 snRNP proteins were transiently expressed in HeLa cells and immunoprecipitated (IP) by using anti-GFP antibodies. Co-precipitated proteins were assayed by western blotting. Non-transfected cells were used as a negative control (−). (C) Endogenous U1-70K was immunoprecipitated from cell lysates and co-precipitated proteins were assayed by western blotting. Ctrl, control. (D,E) U1-70K interacts with SMN in gems. (D) Cells were transiently co-transfected with U1-70K–CFP or U1C–CFP and SMN–YFP. YFP was bleached specifically in gems, and the CFP fluorescence was measured before and after bleaching. a.u., arbitrary units. Scale bars: 5 µm, insets are magnified 2×. (E) FRET efficiency was measured in three independent biological replicates, each containing at least ten cells. Data show the mean±s.e.m. SMN self-interaction was used as a positive control, and empty CFP with SMN–YFP served as a negative control.

the SMN complex through protein–protein interactions independently of the U1 snRNA.

It was recently shown that the protein FUS interacts with both SMN and the U1 snRNP. FUS has been proposed to bridge the SMN complex with the U1 snRNP, but the interaction between the SMN complex and the U1 snRNP has not been directly tested (Yamazaki et al., 2012). Here, we showed that FUS depletion by RNA interference (RNAi) did not interfere with the association between U1-70K and SMN (supplementary material Fig. S2C).

To probe whether U1-70K interacts with SMN in gems, we employed Förster resonance energy transfer (FRET), which has been utilized previously to detect snRNP interaction partners in Cajal bodies (Staněk and Neugebauer, 2004; Huranová et al., 2009). We expressed YFP-tagged SMN protein together with CFP-tagged U1-70K and measured for increased CFP fluorescence after YFP bleaching (Fig. 1D). FRET efficiency between U1-70K and SMN in gems was comparable to FRET signals detected between SMN proteins (Dundr et al., 2004), which was used as a positive control, whereas FRET between SMN and the non-interacting U1C was at the background level (Fig. 1E). These FRET data show that U1-70K associates with SMN in gems.

Interaction between U1-70K and the SMN complex is mediated by the unstructured N-terminal part of U1-70K

Next, we addressed which part of U1-70K interacts with the SMN complex. We found that the SMN complex interaction domain lies in the N-terminal half (amino acids 1–200) of U1-70K

Journal of Cell Science (2014) 127, 3909–3915 doi:10.1242/jcs.155838

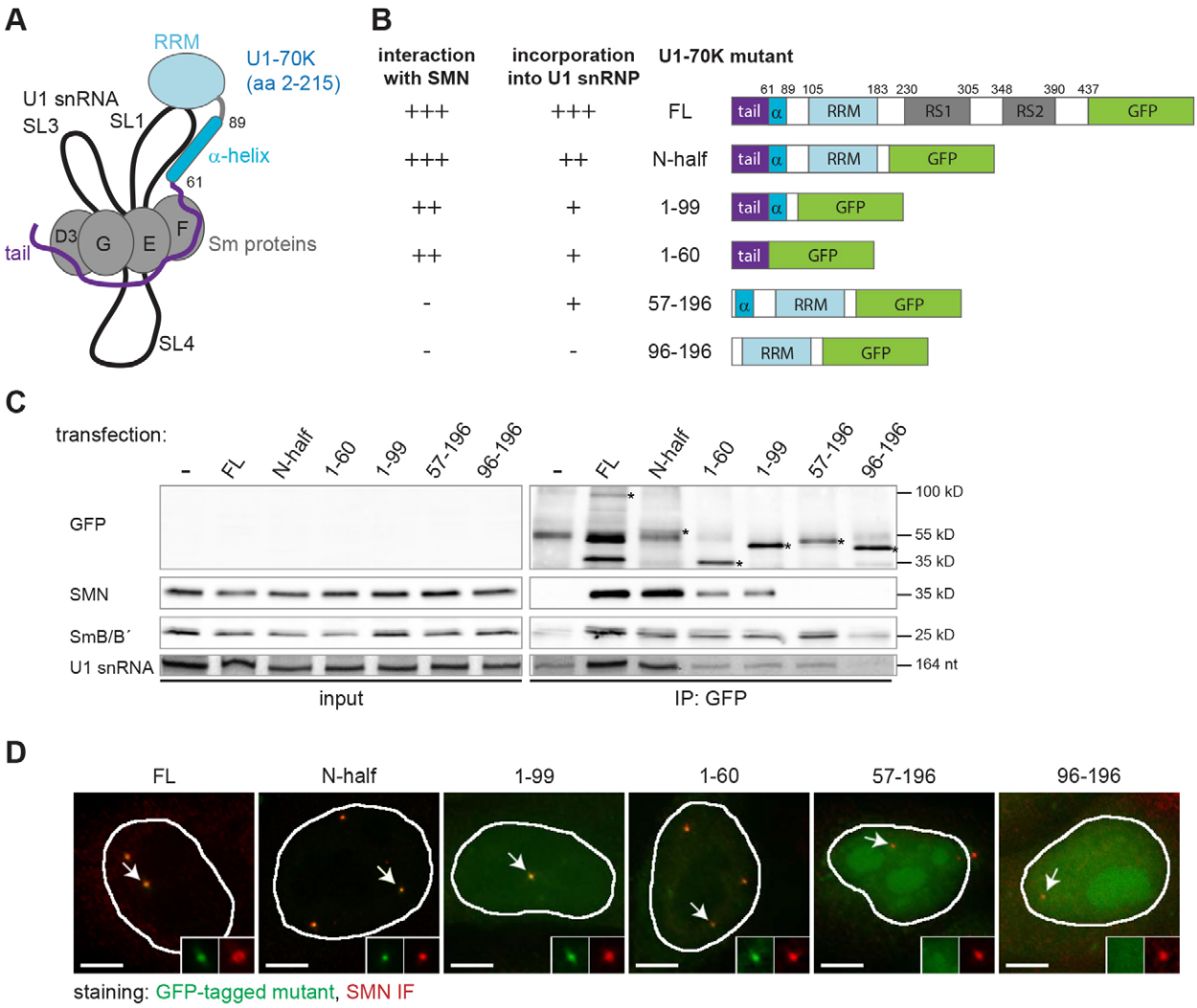

Fig. 2. The N-terminal tail of U1-70K interacts with SMN. (A) A schematic representation of the U1-70K N-terminal half within the U1 snRNP, based on Pomeranz Krummel et al., 2009. SL, stem loop; aa, amino acids. (B) A schematic representation of the U1-70K deletion constructs used in this study. FL, full length; N-half, N-terminal half. (C) Transiently transfected GFP-tagged U1-70K mutants were immunoprecipitated (IP) using anti-GFP antibodies, and co-precipitated proteins and the U1 snRNA were visualized by western blotting and silver staining, respectively. Non-transfected cells served as a negative control (−). Protein bands with correct size are marked by asterisks. The band around 55 kDa corresponds to antibody heavy chains. (D) HeLa cells expressing GFP-tagged U1-70K mutants (green) stained with the anti-SMN antibody (red) marking nuclear gems. Details of selected gems (marked by arrows) are shown in insets. Nuclear outlines are shown in white. IF, immunofluorescence. Scale bars: 5 μm, insets are magnified 2.5×.

(Fig. 2; data not shown). The N-terminal half contains an RNA recognition motif (RRM), α-helical region and the unstructured N-terminal tail (Fig. 2A). The RRM and the α-helical region bind to the U1 snRNA stem loop 1, and the unstructured tail interacts with Sm ring proteins (Stark et al., 2001; Pomeranz Krummel et al., 2009). To further define the SMN-interacting domain, we tagged four different parts of the N-terminal half of U1-70K with GFP (Fig. 2B), expressed them in HeLa cells and immunoprecipitated using anti-GFP antibodies. The co-precipitated SMN protein was detected by western blotting as a marker of the SMN complex (Fig. 2C).

The minimal domain of U1-70K that interacted with the SMN complex consisted of the first 60 amino acids and correlated with the gem-targeting domain (Fig. 2D). By contrast, the mutant lacking the first 60 amino acids and containing the α-helix and RRM was not able to co-precipitate the SMN complex and did not accumulate in gems. However, the α-helix and RRM domain still interacted with the U1 snRNP, as indicated by co-precipitation of the Sm proteins and the U1 snRNA (Fig. 2C, lower panels). These results show that U1-70K incorporation into the U1 snRNP does not correlate with U1-70K interaction with the SMN complex, indicating that U1-70K–SMN association is not mediated by other U1 snRNP components.

In addition to its role in snRNP biogenesis, the SMN complex was suggested to be directly involved in *in vitro* pre-mRNA splicing or recycling of post-spliceosomal complexes (Meister et al., 2000). Moreover, the SMN complex was recently identified in the early spliceosomal complexes (Makarov et al., 2012). U1-70K is a core splicing protein found specifically in early splicing complexes (Will and Luhrmann, 2011). Our data provide a direct link between the SMN complex and early spliceosomes and could explain how the SMN complex associates with the spliceosome.

The U1-70K N-terminal tail is important for gem integrity

To test whether U1-70K is important for gem integrity, we depleted U1-70K by RNAi and stained for SMN (supplementary

Journal of Cell Science (2014) 127, 3909–3915 doi:10.1242/jcs.155838

material Fig. S2D). Nuclear gems disappeared after U1-70K knockdown, and SMN localized diffusely in the cytoplasm and the nucleus. We tested two different small interfering (si)RNAs against U1-70K in three different cell lines and, in all cases, gem number decreased after the siRNA treatment (Fig. 3A; data not shown). To quantify the phenotype, we employed high-content microscopy, which revealed that U1-70K depletion reduced the average number of gems per cell in HeLa KN (Hebert et al., 2002), U2OS and HepG2 cells, whereas Cajal body number was not significantly affected (Fig. 3B; supplementary material Fig. S2G). As reported previously, we observed Cajal body and gem loss after SMN knockdown (Fig. 3B; supplementary material Fig. S2G). Cajal body reduction after SMN knockdown was previously connected with impaired snRNP biogenesis (Shpargel and Matera, 2005; Girard et al., 2006; Lemm et al., 2006). Because Cajal body number was not changed after U1-70K knockdown, we suggest that U1-70K downregulation does not affect snRNP biogenesis. The expression of the SMN protein was not reduced after the knockdown of U1-70K (supplementary material Fig. S2D), indicating that the gem loss was not due to downregulation of the SMN protein. To test whether U1-70K is important for the integrity of the SMN complex, we knocked down U1-70K and analyzed the Gemins that co-precipitated with SMN (Fig. 3C). All of the tested components of the SMN complex co-purified with the SMN protein to a similar extent as in cells treated with a negative control siRNA, which suggests that gem loss is not due to the disintegration of the SMN complex.

To confirm the role of U1-70K in gem formation, we expressed siRNA-resistant U1-70K mutants and analyzed gem formation after U1-70K downregulation (Fig. 4A,C). The expression of the full-length protein, its N-terminal half or the first 1–60 amino acids, all of which interact with the SMN complex (see Fig. 2), rescued the average number of gems, which increased to almost 70% of the original value. By contrast, the mutant 57–196, which does not bind to the SMN complex, was unable to rescue the phenotype above that observed following expression of the empty GFP control. These results suggest that the N-terminal fragment of the U1-70K protein, which interacts with the SMN complex, is important for gem integrity. To test whether the loss of U1-70K can be compensated for by SMN overexpression, we ectopically expressed SMN–YFP, which rescued gem formation (Fig. 4B,D). This result suggests that U1-70K induces gems indirectly, e.g. by increasing a local concentration of SMN or by enhancing the oligomerization properties of SMN.

Taken together, here, we identify U1-70K as an SMN complex interaction partner, which is required for gem formation. It was recently shown that several proteins involved in amyotrophic lateral sclerosis, such as TDP43 and FUS, are important for gem formation (Shan et al., 2010; Kariya et al., 2012; Yamazaki et al., 2012; Tsuiji et al., 2013). As far we know, no mutation of U1-70K has been connected with amyotrophic lateral sclerosis to date (Finsterer and Burgunder, 2014). However, our findings suggest a potential link between U1-70K and neurodegenerative diseases, and U1-70K mutations might be a potential target for screening in

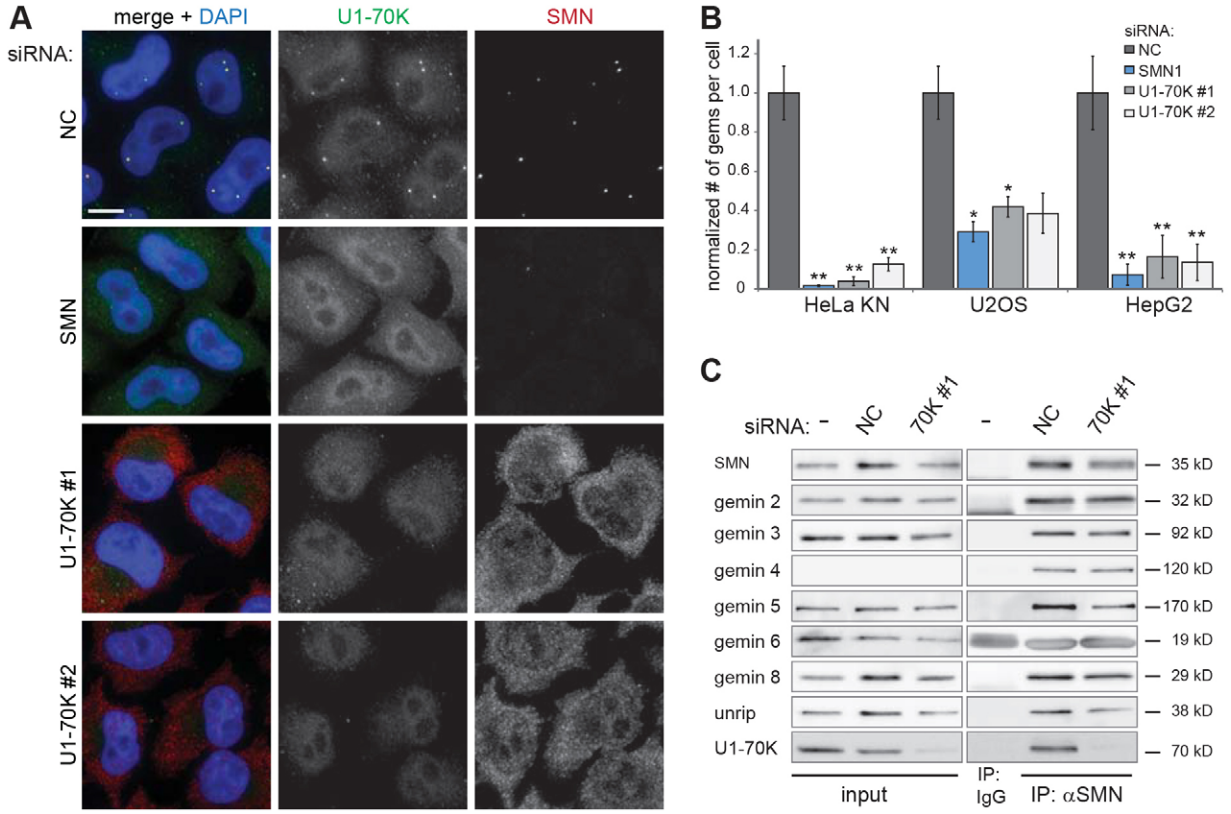

Fig. 3. U1-70K knockdown causes loss of nuclear gems. (A) U1-70K depletion causes loss of nuclear gems (which are marked by SMN staining, red). Two different siRNAs against U1-70K showed the same phenotype, SMN knockdown served as a positive control. Scale bar: 10 μm. See supplementary material Fig. S2D for data on knockdown efficiency. (B) Quantification of the U1-70K knockdown phenotype by high-content microscopy using three different cell lines. The anti-SMN antibody was used to mark gems. The data show the mean±s.e.m. (three experiments, each containing hundreds of cells); *$P \leq 0.05$, **$P \leq 0.01$ against cells treated with negative control (NC) siRNA; Student's *t*-test. (C) SMN complex integrity after U1-70K depletion. Endogenous SMN protein was immunoprecipitated (IP) from HeLa cells that were treated with U1-70K-specific siRNA, and co-precipitated proteins were assayed by western blotting.

Journal of Cell Science (2014) 127, 3909–3915 doi:10.1242/jcs.155838

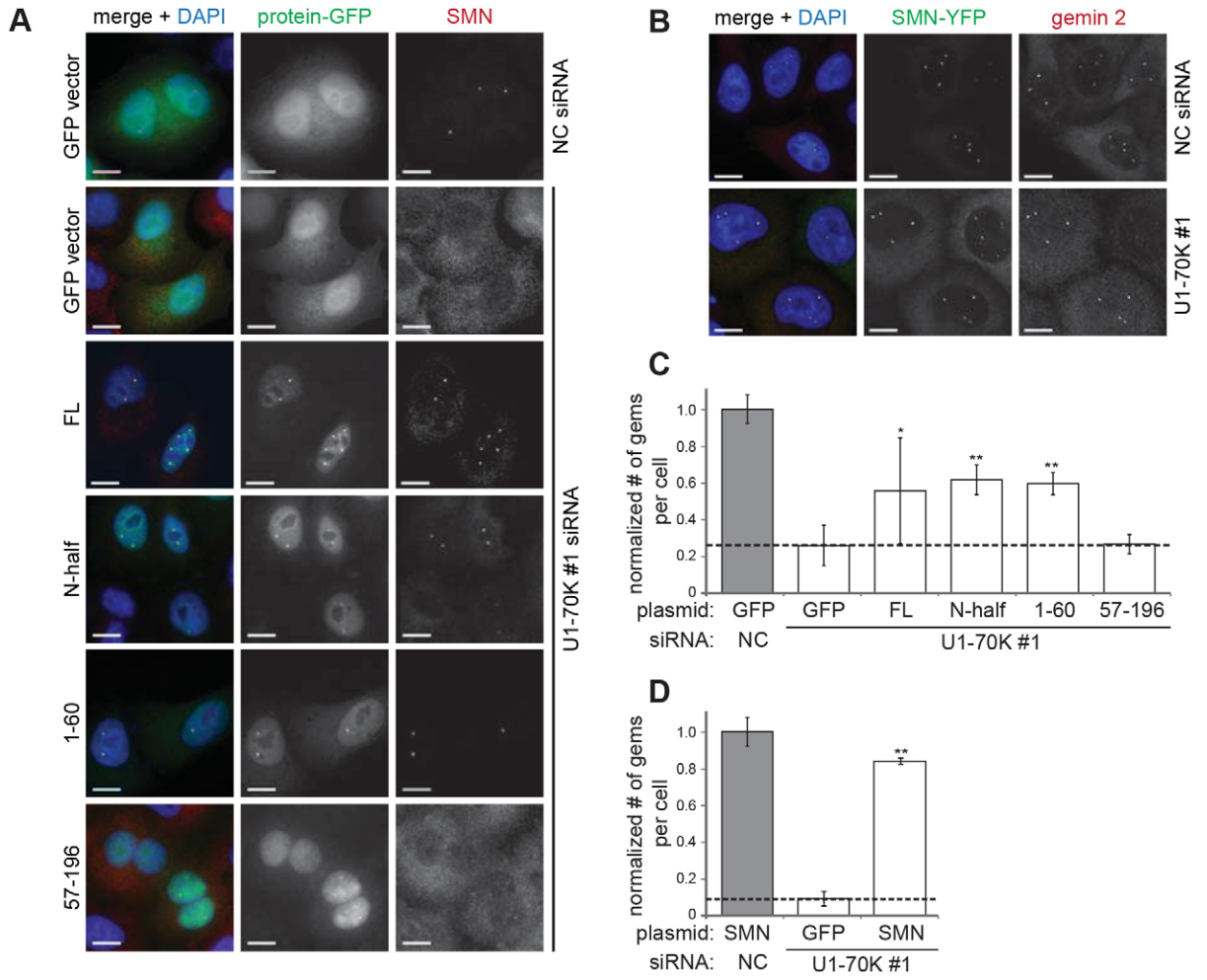

Fig. 4. Nuclear gems are rescued by the ectopic expression of the U1-70K N-terminal tail or by the SMN protein. (A,B) Cells treated with U1-70K siRNA or negative control (NC) siRNA were transiently transfected with GFP-tagged U1-70K mutant constructs (A) or SMN–YFP (green, B) and stained with the anti-SMN (A) or anti-Gemin 2 (B) antibody (red) to mark nuclear gems. FL, full length; N-half, N-terminal half. Scale bars: 10 µm. All U1-70K–GFP constructs were resistant to the siRNA used. See supplementary material Fig. S2E,F for data on knockdown efficiencies. (C,D) Gems were quantified by high-content microscopy. Only cells expressing similar levels of fluorescent proteins were analyzed. The data show the mean±s.e.m. (three experiments, each containing ≥100 cells); **P*≤0.05, ***P*≤0.01 against the empty GFP vector; Student's *t*-test.

the sporadic amyotrophic lateral sclerosis patients who have an unidentified genetic basis of disease.

MATERIALS AND METHODS

Plasmid construction

Full-length U1-70K–GFP was described previously (Huranová et al., 2010). U1A–GFP and U1C–GFP (or CFP) were amplified from cDNA and inserted into the pEGFP-N1 (or pECFP-N1) vectors (Clontech, Mountain View, CA) using the *EcoR*I/*BamH*I and *Xho*I/*EcoR*I restriction sites, respectively. U1-70K–CFP was generated by recloning the U1-70K sequence from full-length U1-70K-GFP into pECFP-N1 using the *EcoR*I/*BamH*I restriction sites. The U1-70K GFP-tagged mutants were generated by PCR amplification of the desired sequences and subsequent cloning into pEGFP-N1 using the *EcoR*I/*BamH*I restriction sites. Two silent point mutations, G414A and G417T, were introduced into the siRNA-binding site of U1-70K by site-directed mutagenesis to generate siRNA-resistant constructs. SMN-CFP-C1 was a gift from Miroslav Dundr (Dundr et al., 2004).

Cell culture and transfections

Cell lines were maintained in DMEM supplemented with 10% fetal calf serum and 1× penicillin-streptomycin (Invitrogen, Carlsbad, CA). We used two different HeLa subclones – HeLa Kyoto and HeLa KN (Hebert et al., 2002). Unless specified otherwise, all experiments were performed using HeLa KN cells.

Plasmids were transfected by using Lipofectamine LTX (Invitrogen), and cells were assayed 24 h after transfection. siRNAs (Ambion, Austin, TX) were transfected using Oligofectamine (Invitrogen) according to the manufacturer's instructions and assayed after 48 h. The siRNA sequences are as follows: U1-70K siRNA#1, 5′-GGUCUACAGUAAGCGGUCATT-3′ (s13211); U1-70K siRNA#2, 5′-CGGACCUAUCAAAAGAAUATT-3′ (s13212); FUS siRNA, 5′-AGCCCAUGAUUAAUUUGUATT-3′ (s5401). Ambion negative control siRNA #5 was used. SMN esiRNA (EHU148811) was from Sigma Aldrich (St Louis, MO).

Antibodies

Primary antibodies used in this study were against: Gemin 2 (clone 3F8) and GFP [clone B-2 (western blotting)] (both from Santa Cruz Biotechnology, Santa Cruz, CA); Gemin 3, Gemin 4 (clone 3E1), Gemin 6, Gemin 8, unrip, SMN1 [clones 2B1 (immunofluorescence, immunoprecipitation) and 2B11 (western blotting)] and FUS (all from Sigma Aldrich); U1-70K [Sigma Aldrich (immunofluorescence, western blotting); Santa Cruz Biotechnology (immunoprecipitation)]; Gemin 5 (clone 10G11; Millipore, Temecula, CA); β-actin (Abcam, Cambridge, UK); coilin (clone 5P10; from Maria Carmo-Fonseca, Instituto de

Medicina Molecular, Lisbon, Portugal). Antibody against SmB/B′ was produced in the Institute of Molecular Genetics antibody facility from a hybridoma cell line obtained from Karla Neugebauer (Yale University, New Haven, CT). Anti-GFP antibodies (immunoprecipitation) were obtained from David Drechsel (Max Planck Institute of Molecular Cell Biology and Genetics, Dresden, Germany).

Secondary antibodies conjugated to DyLight 488, DyLight 549 or Cy5 were used for immunofluorescence staining, and secondary antibodies conjugated to horseradish peroxidase (Jackson ImmunoResearch Laboratories, West Grove, PA) were used for western blotting.

Fixed-cell staining and image acquisition

Cells were fixed and labeled, and images were acquired as described previously (Novotný et al., 2011). U1 snRNA was visualized by fluorescent *in situ* hybridization as described previously (Schaffert et al., 2004). High-content microscopy was performed as described previously (Novotny et al., 2012). FRET measurement by acceptor photobleaching was performed as described previously (Staněk and Neugebauer, 2004).

For super-resolution microscopy, samples were stained as described above and mounted in anti-fade mounting medium [5% (w/v) n-propyl gallate in 20 mM Tris-HCl pH 8.5 in 86% glycerol (optical grade)]. Acquisition was performed on the Delta Vision OMX (Applied Precision, Issaquah, WA), equipped with three-dimensional structured illumination (3D-SIM) and a 60× 1.42 NA objective. 0.125-µm optical sections were acquired. For image reconstruction, we used SoftWorx software implemented with the 3D SI Reconstruction function. Reconstructed images were processed and analyzed using ImageJ software.

Immunoprecipitation

Immunoprecipitation was performed as described previously (Huranová et al., 2009). RNA was extracted using phenol:chloroform, resolved on a 7 M urea denaturing polyacrylamide gel and silver stained. Proteins were resolved by SDS-PAGE and detected by western blotting.

Acknowledgements

We are grateful to Karla Neugebauer, Maria Carmo-Fonseca, Miroslav Dundr and David Drechsel for reagents. We thank Jan Peychl (Max Planck Institute of Molecular Cell Biology and Genetics, Dresden, Germany) and Euro-BioImaging initiative for support with super-resolution microscopy. We are grateful to Kim Kotovic for language proofreading.

Competing interests

The authors declare no competing interests.

Author contributions

E.S. and D.S. conceived and designed the experiments; E.S. performed the experiments and analyzed the data; E.S. and D.S. wrote the paper.

Funding

This work was supported by the Czech Science Foundation [grant number P302/11/1910]; the Academy of Sciences of the Czech Republic [grant numbers RVO68378050 and M200521206]; and the Grant Agency of Charles University [grant number 320713 to E.S.].

Supplementary material

Supplementary material available online at
http://jcs.biologists.org/lookup/suppl/doi:10.1242/jcs.155838/-/DC1

References

Achsel, T., Barabino, S., Cozzolino, M. and Carrì, M. T. (2013). The intriguing case of motor neuron disease: ALS and SMA come closer. *Biochem. Soc. Trans.* **41**, 1593-1597.

Carmo-Fonseca, M., Pepperkok, R., Sproat, B. S., Ansorge, W., Swanson, M. S. and Lamond, A. I. (1991). In vivo detection of snRNP-rich organelles in the nuclei of mammalian cells. *EMBO J.* **10**, 1863-1873.

Cauchi, R. J. (2010). SMN and Gemins: 'We are family' … or are we? Insights into the partnership between Gemins and the spinal muscular atrophy disease protein SMN. *Bioessays* **32**, 1077-1089.

Dundr, M., Hebert, M. D., Karpova, T. S., Staněk, D., Xu, H., Shpargel, K. B., Meier, U. T., Neugebauer, K. M., Matera, A. G. and Misteli, T. (2004). In vivo kinetics of Cajal body components. *J. Cell Biol.* **164**, 831-842.

Finsterer, J. and Burgunder, J. M. (2014). Recent progress in the genetics of motor neuron disease. *Eur. J. Med. Genet.* **57**, 103-112.

Fischer, U. and Lührmann, R. (1990). An essential signaling role for the m3G cap in the transport of U1 snRNP to the nucleus. *Science* **249**, 786-790.

Fischer, U., Sumpter, V., Sekine, M., Satoh, T. and Lührmann, R. (1993). Nucleo-cytoplasmic transport of U snRNPs: definition of a nuclear location signal in the Sm core domain that binds a transport receptor independently of the m3G cap. *EMBO J.* **12**, 573-583.

Fischer, U., Liu, Q. and Dreyfuss, G. (1997). The SMN-SIP1 complex has an essential role in spliceosomal snRNP biogenesis. *Cell* **90**, 1023-1029.

Fischer, U., Englbrecht, C. and Chari, A. (2011). Biogenesis of spliceosomal small nuclear ribonucleoproteins. *Wiley Interdiscip. Rev. RNA* **2**, 718-731.

Girard, C., Neel, H., Bertrand, E. and Bordonné, R. (2006). Depletion of SMN by RNA interference in HeLa cells induces defects in Cajal body formation. *Nucleic Acids Res.* **34**, 2925-2932.

Grimmler, M., Otter, S., Peter, C., Müller, F., Chari, A. and Fischer, U. (2005). Unrip, a factor implicated in cap-independent translation, associates with the cytosolic SMN complex and influences its intracellular localization. *Hum. Mol. Genet.* **14**, 3099-3111.

Hebert, M. D., Shpargel, K. B., Ospina, J. K., Tucker, K. E. and Matera, A. G. (2002). Coilin methylation regulates nuclear body formation. *Dev. Cell* **3**, 329-337.

Huranová, M., Hnilicová, J., Fleischer, B., Cvacková, Z. and Staněk, D. (2009). A mutation linked to retinitis pigmentosa in HPRP31 causes protein instability and impairs its interactions with spliceosomal snRNPs. *Hum. Mol. Genet.* **18**, 2014-2023.

Huranová, M., Ivani, I., Benda, A., Poser, I., Brody, Y., Hof, M., Shav-Tal, Y., Neugebauer, K. M. and Staněk, D. (2010). The differential interaction of snRNPs with pre-mRNA reveals splicing kinetics in living cells. *J. Cell Biol.* **191**, 75-86.

Kariya, S., Re, D. B., Jacquier, A., Nelson, K., Przedborski, S. and Monani, U. R. (2012). Mutant superoxide dismutase 1 (SOD1), a cause of amyotrophic lateral sclerosis, disrupts the recruitment of SMN, the spinal muscular atrophy protein to nuclear Cajal bodies. *Hum. Mol. Genet.* **21**, 3421-3434.

Lemm, I., Girard, C., Kuhn, A. N., Watkins, N. J., Schneider, M., Bordonné, R. and Lührmann, R. (2006). Ongoing U snRNP biogenesis is required for the integrity of Cajal bodies. *Mol. Biol. Cell* **17**, 3221-3231.

Liu, Q. and Dreyfuss, G. (1996). A novel nuclear structure containing the survival of motor neurons protein. *EMBO J.* **15**, 3555-3565.

Machyna, M., Heyn, P. and Neugebauer, K. M. (2013). Cajal bodies: where form meets function. *Wiley Interdiscip. Rev. RNA* **4**, 17-34.

Makarov, E. M., Owen, N., Bottrill, A. and Makarova, O. V. (2012). Functional mammalian spliceosomal complex E contains SMN complex proteins in addition to U1 and U2 snRNPs. *Nucleic Acids Res.* **40**, 2639-2652.

Malatesta, M., Scassellati, C., Meister, G., Plöttner, O., Bühler, D., Sowa, G., Martin, T. E., Keidel, E., Fischer, U. and Fakan, S. (2004). Ultrastructural characterisation of a nuclear domain highly enriched in survival of motor neuron (SMN) protein. *Exp. Cell Res.* **292**, 312-321.

Massenet, S., Pellizzoni, L., Paushkin, S., Mattaj, I. W. and Dreyfuss, G. (2002). The SMN complex is associated with snRNPs throughout their cytoplasmic assembly pathway. *Mol. Cell. Biol.* **22**, 6533-6541.

Matera, A. G. and Ward, D. C. (1993). Nucleoplasmic organization of small nuclear ribonucleoproteins in cultured human cells. *J. Cell Biol.* **121**, 715-727.

Meister, G., Bühler, D., Laggerbauer, B., Zobawa, M., Lottspeich, F. and Fischer, U. (2000). Characterization of a nuclear 20S complex containing the survival of motor neurons (SMN) protein and a specific subset of spliceosomal Sm proteins. *Hum. Mol. Genet.* **9**, 1977-1986.

Narayanan, U., Achsel, T., Lührmann, R. and Matera, A. G. (2004). Coupled in vitro import of U snRNPs and SMN, the spinal muscular atrophy protein. *Mol. Cell* **16**, 223-234.

Navascues, J., Berciano, M. T., Tucker, K. E., Lafarga, M. and Matera, A. G. (2004). Targeting SMN to Cajal bodies and nuclear gems during neuritogenesis. *Chromosoma* **112**, 398-409.

Neuman de Vegvar, H. E. and Dahlberg, J. E. (1990). Nucleocytoplasmic transport and processing of small nuclear RNA precursors. *Mol. Cell. Biol.* **10**, 3365-3375.

Novotný, I., Blažíková, M., Staněk, D., Herman, P. and Malinsky, J. (2011). In vivo kinetics of U4/U6·U5 tri-snRNP formation in Cajal bodies. *Mol. Biol. Cell* **22**, 513-523.

Novotny, I., Podolská, K., Blazíková, M., Valásek, L. S., Svoboda, P. and Staněk, D. (2012). Nuclear LSm8 affects number of cytoplasmic processing bodies via controlling cellular distribution of Like-Sm proteins. *Mol. Biol. Cell* **23**, 3776-3785.

Otter, S., Grimmler, M., Neuenkirchen, N., Chari, A., Sickmann, A. and Fischer, U. (2007). A comprehensive interaction map of the human survival of motor neuron (SMN) complex. *J. Biol. Chem.* **282**, 5825-5833.

Pomeranz Krummel, D. A., Oubridge, C., Leung, A. K. W., Li, J. and Nagai, K. (2009). Crystal structure of human spliceosomal U1 snRNP at 5.5 A resolution. *Nature* **458**, 475-480.

Schaffert, N., Hossbach, M., Heintzmann, R., Achsel, T. and Lührmann, R. (2004). RNAi knockdown of hPrp31 leads to an accumulation of U4/U6 di-snRNPs in Cajal bodies. *EMBO J.* **23**, 3000-3009.

Shan, X., Chiang, P. M., Price, D. L. and Wong, P. C. (2010). Altered distributions of Gemini of coiled bodies and mitochondria in motor neurons of TDP-43 transgenic mice. *Proc. Natl. Acad. Sci. USA* **107**, 16325-16330.

Shpargel, K. B. and Matera, A. G. (2005). Gemin proteins are required for efficient assembly of Sm-class ribonucleoproteins. *Proc. Natl. Acad. Sci. USA* **102**, 17372-17377.

Staněk, D. and Neugebauer, K. M. (2004). Detection of snRNP assembly intermediates in Cajal bodies by fluorescence resonance energy transfer. *J. Cell Biol.* **166**, 1015-1025.

Stark, H., Dube, P., Lührmann, R. and Kastner, B. (2001). Arrangement of RNA and proteins in the spliceosomal U1 small nuclear ribonucleoprotein particle. *Nature* **409**, 539-542.

Tsuiji, H., Iguchi, Y., Furuya, A., Kataoka, A., Hatsuta, H., Atsuta, N., Tanaka, F., Hashizume, Y., Akatsu, H., Murayama, S. et al. (2013). Spliceosome integrity is defective in the motor neuron diseases ALS and SMA. *EMBO Mol. Med.* **5**, 221-234.

Will, C. L. and Lührmann, R. (2011). Spliceosome structure and function. *Cold Spring Harb. Perspect. Biol.* **3**, a003707.

Yamazaki, T., Chen, S., Yu, Y., Yan, B., Haertlein, T. C., Carrasco, M. A., Tapia, J. C., Zhai, B., Das, R., Lalancette-Hebert, M. et al. (2012). FUS-SMN protein interactions link the motor neuron diseases ALS and SMA. *Cell Reports* **2**, 799-806.